A New Set Of Analytical Correlations For Predicting Convective Heat Transfer In Fenestration Glazing Cavities

Yie Zhao*, William P. Goss*, Dragan Curcija, Joseph P. Power***

*** Department of Mechanical and Industrial Engineering**

University of Massachusetts, Amherst, MA 01003-2210, U.S.A.

**** CARLI, Inc., 379 Strong St. Suite 200, Amherst, MA 01002, U.S.A.**

ABSTRACT

Analytically modeling the complex fluid flow phenomena that occurs during natural convective heat transfer in fenestration system cavities (windows, doors, skylights, curtain-walls, etc.) is a complex task. Laminar flow of a fluid in a tall vertical glazing cavity can occur in the form of single cell or as a stable multicellular flow. Until the early 1980's, experimental results were mostly available, along with limited analytical studies based on theoretical considerations. Empirical heat transfer correlations, based on experimental results for tall cavities, are still widely used to determine the heat transfer through the fenestration glazing cavities. The correlations currently in use are primarily functions of the Rayleigh number, Ra_L, and sometimes the aspect ratio, A (ratio of cavity height to width). However, the dependence of heat transfer coefficient on the aspect ratio A has not been completely resolved.

In this work, based on the numerical results obtained using finite element calculation methods, a new set of analytical correlations are developed as functions of both Ra_L and A. The numerical analysis was performed over a range of aspect ratios from A=5 to 80 with Rayleigh numbers within the laminar flow regime, which covers a range of conditions typical of fenestration systems and solar energy collectors. The standard deviation between the numerical results and the analytical correlations developed from them is less 2 than percent. The new correlations are also in good agreement with available experimental data and other numerical calculations as shown in the results and discussion section. The new correlation is formulated as two equations applicable for two ranges of Rayleigh numbers, making them easy to use in engineering practice.

INTRODUCTION

Convective heat transfer in insulated glazing unit (IGU) cavities is a major component of the overall heat transfer in fenestration systems. The present understanding of the thermal and hydrodynamic behavior of natural convection heat transfer in enclosures is based on the experimental studies of Eckert and Carlson (1961) and Elder (1965). These two studies provided detailed measurements of the velocity and temperature distributions in cavities, making the thermal and hydrodynamic behavior better understood. They also confirmed the existence of the flow regimes described in an earlier analytical investigation of Batchelor (1954), who had concluded that the two regimes that exist in the flow field were: (1) at low Ra_L, heat is transferred across the cavity primarily by conduction, and (2) at high Ra_L, the flow is confined to boundary layers at the side walls for which the dominant mode of heat transfer is convection. These two flow situations are called the conduction regime and the boundary layer regime. Contrary to the Batchelor's uniform temperature core suggestion (1954) for the boundary layer regime, Eckert and Carlson (1961) and Elder (1965) observed a presence of a vertical

temperature gradient in the core region for flow beyond the conduction regime. As an enhancement of the two regimes defined by Batchelor (1954), three heat transfer regimes were qualitatively defined by Eckert and Carlson (1961). They were the conduction regime, transition regime (between the conduction and boundary layer regimes) and boundary layer regime as shown by a regime definition figure in their paper. In addition, they proposed two correlations to evaluate the heat transfer in the conduction and boundary layer regimes:

Conduction regime correlation:

$$Nu_L = 1 + 0.00166 \times (Gr_L)^{0.9} \times \frac{L}{H} \quad (1)$$

Boundary layer regime correlation:

$$Nu_L = 0.119 \times (Gr_L)^{0.3} \times (\frac{L}{H})^{0.1} \quad (2)$$

Since the number of experiments conducted by Eckert and Carlson was not sufficient to quantitatively establish the exact limits between the various heat transfer regimes as well as to quantify the heat transfer performance in the transition regime, the above two correlation equations are restricted to the conduction regime and boundary layer regime, whose limits are shown in a flow regime definition figure given in Eckert and Carlson (1961).

Since these early pioneer studies, a number of numerical and experimental studies have been conducted for natural convection in air filled rectangular vertical cavities and slots. Jakob (1967) developed a correlation based on early experimental studies of natural convection in rectangular cavities for the aspect ratios between 3.12 and 42.2. Newell and Schmidt (1970) solved the time dependent governing differential equations (mass, momentum and energy) by using Crank and Nicholson finite difference method. Yin, et al (1978) experimentally investigated natural convection for various cavity aspect ratios ranging from 4.9 to 78.7. All of the correlations that were developed to evaluate the heat transfer across vertical cavities had the same form as shown below:

$$Nu_L = C \times (Gr_L)^a \times (\frac{H}{L})^b \quad (3)$$

The numerical values for constants *C*, *a* and *b* are given in Table 1 which also includes the boundary layer regime's correlation of Eckert and Carlson (1961). It should be noted that the correlations given in Table 1 were developed with zero heat flux (ZHF) boundary conditions at top and bottom cavity surfaces, and are for air, with a Prandtl Number, *Pr*, of approximately 0.7.

Table 1 Empirical constants and range of *A* and Gr_L for Equation 3

Investigator	C	a	b	Range of *A*	Range of Gr_L
Jakob	0.180	0.250	-0.111	3.12 to 42.2	2.0×10^4 to 2.0×10^5
Eckert and Carlson	0.119	0.300	-0.100	2.5 to 46.7	Defined in their figure
Newell and	0.155	0.315	-0.265	2.5 to 20.0	4.0×10^3 to 1.4×10^5
Yin et al.	0.210	0.269	-0.131	4.9 to 78.7	1.5×10^3 to 7.0×10^6

To be more general for different fluids, the product of Grashof number and the Prandtl number, the Rayleigh number, Ra_L, should be used. Raithby, et al (1977) presented an analysis for the heat transfer across near vertical fluid cavities with the ZHF boundary conditions at the top and bottom cavity surfaces based on the previous analytical work of Raithby and Hollands (1975). There, a generalized correlation equation set to evaluate the integrated Nusselt number was proposed for fluid layers tilting in the range of -20° to 20° from the vertical and Prandtl numbers varying from 0.02 to ∞. In addition, their correlation covers both the laminar and turbulent flow regimes. For air filled vertical cavities, their correlation consists of three equations where the maximum value of the Nusselt number from the three equations shown below is used. The value of one is the lower limit for conduction only.

$$Nu_L = \left\{ \begin{array}{l} 1 \\ 0.2881 \times \left(\dfrac{Ra_L}{A} \right)^{0.25} \\ 0.0395 \times Ra_L{}^{\frac{1}{3}} \end{array} \right\}_{\max} \tag{4}$$

The above equation set is valid for aspect ratios greater than 5 and Rayleigh numbers varying from 10^3 to approximately 7×10^6 (this range of Rayleigh numbers was obtained from their figures (Raithby, et al 1977). For higher aspect ratios, when compared with the experimental data of ElSherbiny, et al (1982), Equation 4 underpredicts the integrated Nusselt number from 9% at A=40 to 28% at A=80 for a large range of Rayleigh numbers.

All of the correlations reviewed so far are simple power law type of equations, which are unable to account for the complex interaction of aspect ratios and Rayleigh numbers on integrated Nusselt numbers. As a result, discrepancies exist between different correlations, and also between correlations and experimental data. To overcome this problem, more comprehensive forms of the correlation equations have been used since early 1980's. Raithby and Wong (1981) developed a correlation based on their numerical results, using the finite difference method, for vertically oriented air filled cavities. Their correlation, as given below, is valid for aspect ratios from 2 to 80 and Rayleigh numbers from 10^3 to 10^5:

$$Nu_L = \left(1 + \left(\frac{0.334 (Ra^*)^{0.25}}{1 + \dfrac{112}{(Ra^*)^{0.87}}} \right)^2 \right)^{0.5} \tag{5}$$

Where Ra^* for cavities with perfectly conducting boundary conditions at the cavity top and bottom boundaries, called the linear temperature profile (LTP) boundary condition, is given by:

$$Ra^* = \left(1 - \frac{1.02}{A^{0.44}}\right) \frac{Ra_L}{A} \tag{6a}$$

For cavities with zero heat flux boundary conditions at the cavity top and bottom boundaries, called the zero heat flux (ZHF) boundary condition, Ra^* is given by:

$$Ra^* = (0.89 - \frac{0.73}{A})\frac{Ra_L}{A} \tag{6b}$$

ElSherbiny, et al (1982) performed experimental studies for cavities with perfectly conducting top and bottom cavity boundaries (LTP conditions), which resulted in six correlations, one for each aspect ratio (A=5, 10, 20, 40, 80, 110). Except for the correlation at A=20, the other five equations are considered the most accurate presented to date, but are restricted to the corresponding aspect ratios only. To overcome this shortcoming, ElSherbiny, et al (1982) also provided a correlation applicable over the range of aspect ratios and Rayleigh numbers for their measurements. This correlation, because it is much simpler then the six equations for the specific aspect ratios, compromises some accuracy due to the large range of aspect ratios and Rayleigh numbers it covers. Their correlation has the following form :

$$Nu_L = \left\{ \begin{array}{l} 0.0605 Ra_L^{1/3} \\ \{1 + [0.104 Ra_L^{0.293} / (1 + (6310 / Ra_L)^{1.36})]^3\}^{1/3} \\ 0.242 (Ra_L / A)^{0.272} \end{array} \right\}_{\max} \tag{7}$$

Where again, the maximum value of the Nusselt number from the three equations is used. It can be observed that only the third equation in this set of equation is a function of the aspect ratio and it only affects the Nu_L if A is less than 20.

More recently, Wright (1996) developed a new correlation from the experimental data of ElSherbiny, et al (1982) and Shewen (1986), both of which has the LTP boundary conditions at the top and bottom cavity surfaces. Wright's correlation has the form:

$$Nu_L = \left\{ \begin{array}{l} Nu_{L1} = \left(\begin{array}{ll} 0.0673838 Ra_L^{1/3} & for\ Ra_L > 5 \times 10^4 \\ 0.028154 Ra_L^{0.4134} & for\ 10^4 < Ra_L \le 5 \times 10^4 \\ 1 + 1.75967 \times 10^{-10}\, Ra_L^{2.2984755} & for\ Ra_L < 10^4 \end{array} \right) \\ \\ Nu_{L2} = 0.242 (\frac{Ra_L}{A})^{0.272} \end{array} \right\}_{\max} \tag{8}$$

This correlation is similar to that of ElSherbiny, et al (1982). It includes the correlation Nu_{L1}, which was developed from the experiment data of both ElSherbiny, et al (1982) and Shewen (1986) and the third equation of ElSherbiny's correlation (Equation 7) which is designated as Nu_{L2}. In Equations 8, again the only place where the aspect ratio is included is the last equation. However, the applicable aspect ratio range was improved from $A < 20$ in Equation 7 to $A < 25$ in Equation 8. Hence, for aspect ratios which are greater than 25 and less than 110, the Nu_L is assumed to be independent of the aspect ratio. This is not true for moderately high aspect ratios between 25 and 40, as pointed out by Korpela, et al (1982), who showed that the aspect ratio has fairly significant effect on the integrated Nusselt number. It also appears that for higher aspect ratios in the range of $40 < A < 80$, and for Rayleigh numbers greater than 5950 when multicellular flow patterns exist, the resulting Nusselt number will be dependent on the aspect ratio. The reason is that at higher aspect ratios, more cells will exist in the cavity (Korpela, et al

1982, Lee and Korpela 1983, Quéré 1990, Zhao, et al 1997), therefore increasing the integrated Nusselt number. In addition, based on the limit of transition from the laminar regime to the turbulent regime defined by either Batchelor (1954) or Yin, et al (1978), the higher the aspect ratio, the earlier the flow becomes turbulent. Therefore, it is expected that the values of Nu_L will be different for different aspect ratios at the same Rayleigh number. Actually, it can be shown by using the more accurate set of correlations from ElSherbiny, et al (1982) that the difference in Nusselt numbers between different aspect ratios ($A \geq 40$) could be up to 8 percent at high Rayleigh numbers.

Therefore, in this work, the objective was to develop a set of correlations that are able to more accurately predict natural convection heat transfer in vertical cavities as a function of both aspect ratio and Rayleigh number. To accomplish this, laminar natural convection in insulated glazing unit (IGU) cavities with constant temperature boundary conditions along the vertical surfaces and zero heat flux (ZHF) boundary conditions at the horizontal surfaces was investigated. Numerical calculations were performed for twelve aspect ratios from 5 to 80 and a range of Rayleigh numbers within the laminar flow regime (see hatched area in Figure 1). The numerical calculations were performed by using a general-purpose fluid flow and heat transfer finite-element analysis software package FIDAP (FDI 1996).

In addition to the present range of investigation, the limits of transition from laminar flow to turbulent flow (Yin, et al 1978) and the limit of transition from the conduction regime to boundary layer regime (Batchelor 1954) are also included in Figure 1. It can be observed that the current investigation covers a large range of laminar flow regime, which represents many of the conditions typical for fenestration systems and solar energy collectors. For A=80, the limit of transition to turbulent flow was attained.

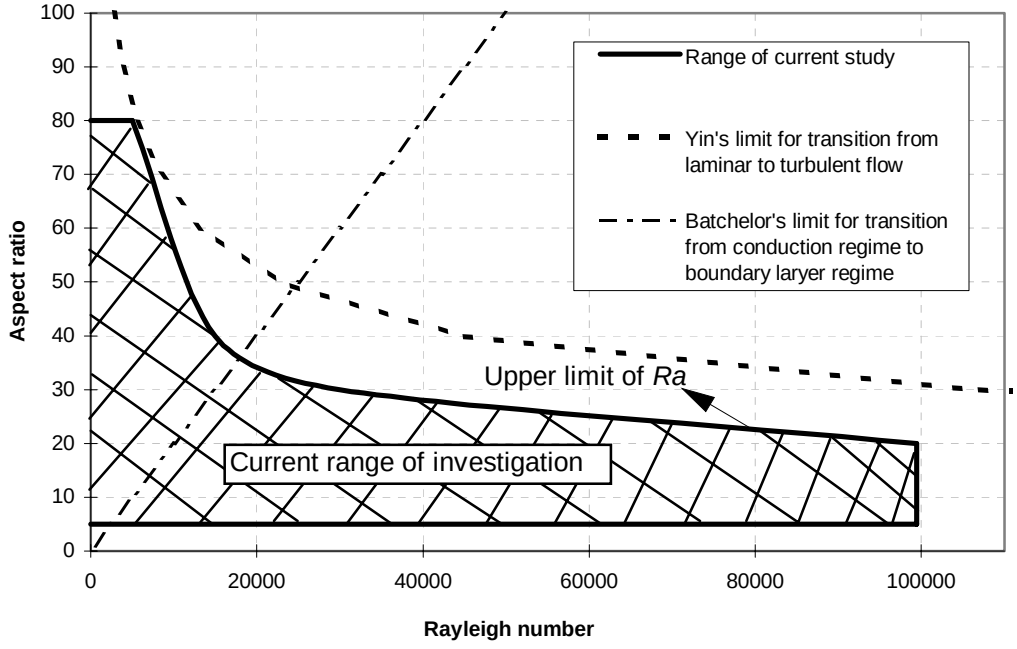

Figure 1. Range of aspect ratios and Rayleigh numbers covered in this study

PROBLEM DESCRIPTION

The geometry and boundary conditions for an IGU cavity typical of fenestration systems is shown in Figure 2. To treat the problem as two-dimensional (2-D), it is assumed that the cavity is infinitely long in the z-direction which is perpendicular to the plane of the drawing. The two vertical walls are held at constant temperatures T_1 and T_0 with $T_1 > T_0$. The top and bottom walls are adiabatic (ZHF conditions).

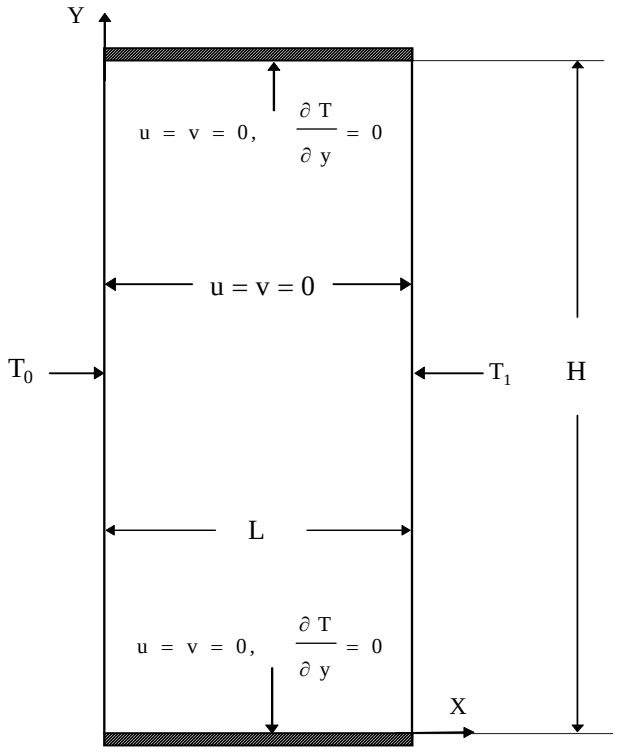

Figure 2. Geometry and boundary conditions for IGU rectangular cavity.

Laminar natural convective heat transfer is governed by the fundamental laws of conservation of mass (continuity equation), Newton's Second law (momentum equation) and the conservation of energy (energy equation). For the two-dimensional problem considered here, following the Boussinesq approximation as well as the assumption of an incompressible fluid flow with negligible viscous dissipation, the dimensionless form of the governing equations can be given as,

Continuity equation: $$\frac{\partial u}{\partial x} + \frac{\partial v}{\partial y} = 0 \qquad (9)$$

Momentum equations:

x direction: $$\sqrt{\frac{Ra_L}{\mathrm{Pr}}}\left[\frac{\partial u}{\partial t}+u\frac{\partial u}{\partial x}+v\frac{\partial u}{\partial y}\right]=-\frac{\partial p}{\partial x}+\left[\frac{\partial^2 u}{\partial x^2}+\frac{\partial^2 u}{\partial y^2}\right] \quad (10)$$

y direction: $$\sqrt{\frac{Ra_L}{\mathrm{Pr}}}\left[\frac{\partial v}{\partial t}+u\frac{\partial v}{\partial x}+v\frac{\partial v}{\partial y}\right]=-\frac{\partial p}{\partial y}+\left[\frac{\partial^2 v}{\partial x^2}+\frac{\partial^2 v}{\partial y^2}\right]-\sqrt{\frac{Ra_L}{\mathrm{Pr}}}\Theta \quad (11)$$

Energy equation: $$\mathrm{Pr}\sqrt{\frac{Ra_L}{\mathrm{Pr}}}\left[\frac{\partial \Theta}{\partial t}+u\frac{\partial \Theta}{\partial x}+v\frac{\partial \Theta}{\partial y}\right]=\frac{\partial^2 \Theta}{\partial x^2}+\frac{\partial^2 \Theta}{\partial y^2} \quad (12)$$

The characteristic of velocity, temperature, pressure, length and time used to make the field variables dimensionless are:

$$\mathrm{U},\quad \Delta\mathrm{T},\quad \frac{\mu \mathrm{U}}{\mathrm{L}},\quad \mathrm{L},\quad \mathrm{L}/\mathrm{U} \quad (13)$$

where the characteristic velocity is defined as $\mathrm{U}\equiv(g\beta\Delta\mathrm{TL})^{1/2}$. The boundary conditions imposed in the dimensionless form for this problem are given below.

Temperature boundary conditions on the vertical surfaces:

$$\Theta(\mathrm{x}=0,\mathrm{y})=0,\quad \Theta(\mathrm{x}=1,\ \mathrm{y})=1 \quad (14)$$

No slip velocity boundary conditions on all bounding surfaces:

$$\mathrm{u}(\mathrm{x}=0,\mathrm{y})=\mathrm{v}(\mathrm{x}=0,\mathrm{y})=0,\quad \mathrm{u}(\mathrm{x}=1,\mathrm{y})=\mathrm{v}(\mathrm{x}=1,\mathrm{y})=0 \quad (15)$$

$$\mathrm{u}(\mathrm{x},\mathrm{y}=0)=\mathrm{v}(\mathrm{x},\mathrm{y}=0)=0,\quad \mathrm{u}(\mathrm{x},\mathrm{y}=\mathrm{H})=\mathrm{v}(\mathrm{x},\mathrm{y}=\mathrm{H})=0 \quad (16)$$

Zero heat flux boundary conditions at the top and bottom surfaces:

$$\left.\frac{\partial \Theta}{\partial \mathrm{y}}\right|_{\mathrm{y}=0}=0,\quad \left.\frac{\partial \Theta}{\partial \mathrm{y}}\right|_{\mathrm{y}=\mathrm{H}}=0 \quad (17)$$

NUMERICAL CALCULATIONS

The finite element calculation procedure used in this study is based on the Galerkin Weighted Residual Method (WRM) in which penalty function approach is utilized to reduce the number of unknowns, by eliminating the pressure from the problem. A detailed discussion of this numerical method for the solution of natural convection heat transfer in fenestration system cavities can be found in FDI (1996) and Curcija (1992).

The computational domain considered here is described by a set of fully coupled nonlinear governing equations. Therefore, to assure the convergence of the solution method, an incremental loading technique was applied. This technique consists of initially assuming a Rayleigh number much lower than required so as to obtain a converged solution, and then using this solution as the initial condition (or guess) for the next calculation made at a higher Rayleigh number. The technique is repeated until a converged solution is obtained for the desired Rayleigh number. The purpose of this technique is to bring the initial guess for each load step within the radius of convergence of the numerical iteration method used. In addition, at higher Rayleigh numbers, the flow becomes unsteady and as a result the steady state time independent solutions become

divergent. Therefore, in this study the non-steady (time dependent) forms of the governing equations were solved for higher Rayleigh numbers to insure more appropriate converged solutions.

A numerical finite element grid study, based on methods presented in Burnett (1984), was performed for low (5), middle (20) and high (80) aspect ratios. The type of element selected throughout this study is a 9-node quadrilateral element. Table 2 gives the result of the grid study for three selected aspect ratios.

Table 2. Examples of the grid study results

Finite element numerical results for A=80, Ra_L =5000					
Grid (i×j)	Nu_L	Grid (i×j)	Nu_L	Grid (i×j)	Nu_L
4x120	1.048404	4x178	1.048419	4x210	1.048425
8x120	1.046684	8x178	1.046687	8x210	1.046687
12x120	1.046507	12x178	1.046510	12x210	1.046510
16x120	1.046464	16x178	1.046468	16x210	1.046468
20x120	1.046449	20x178	1.046453	20x210	1.046453
Finite element numerical results for A=20, Ra_L =40000					
4x40	2.258403	4x60	2.084631	4x80	2.104691
8x40	2.078770	8x60	2.073099	8x80	2.073637
12x40	2.095914	12x60	2.066097	12x80	2.067072
16x40	2.094041	16x60	2.064561	16x80	2.065436
Finite element numerical results for A=5, Ra_L =100000					
4x30	4.112123	4x44	4.114562	4x60	4.115644
8x30	3.782898	8x44	3.783152	8x60	3.783269
12x30	3.741630	12x44	3.741682	12x60	3.741708
16x30	3.730722	16x44	3.730753	16x60	3.730760
20x30	3.726700	20x44	3.726730	20x60	3.726739

In Table 2, i×j denotes the number of elements in the x-direction by the number of elements in the y-direction (see Figure 2 for the definition of the x and y directions). It should be noted that the elements are not evenly spaced in the problem domain. Gradual meshing was employed with thinner elements used close to the walls. As it can be seen, increasing the already large number of elements in the y direction has very small effect on Nu_L. On the other hand, increasing the smaller number of elements in x direction has a significant effect for all aspect ratios. Based on the discussions of Gill (1966) and Curcija (1994) for numerical calculations for this type of problem, to obtain accurate results the thickness of the first layer of elements closest

to the vertical wall must be checked with the formula $\delta = L\times(Ra_L\times L/H)^{-0.25}$ for estimating a boundary layer thickness. The mesh refinement should be undertaken whenever the thickness of the first layer of elements is larger than that of δ. The thickness requirement of the first layer of the elements does not apply to flow in the conduction regime as is the case for A=80 and Ra_L =5000, where mesh density variations in the x direction produce very little change in the calculated Nusselt numbers. It should be noted that at certain aspect ratios and values of Ra_L, multicellular flow occurred, resulting in increased heat transfer rates. The limits of this flow are discussed in Zhao, et al (1997). It was found that for the three examples shown in Table 2, 16x178, 12x80 and 12x44 grids are sufficient for performing the numerical calculations for aspect ratios of 80, 20 and 5 respectively. In this study, the appropriate mesh density for those aspect ratios where the grid study was not performed was constructed using the guidance of the known mesh densities at aspect ratios where the grid study was carried out. Examples of finite element meshes for several different aspect ratios are shown in Figure 3.

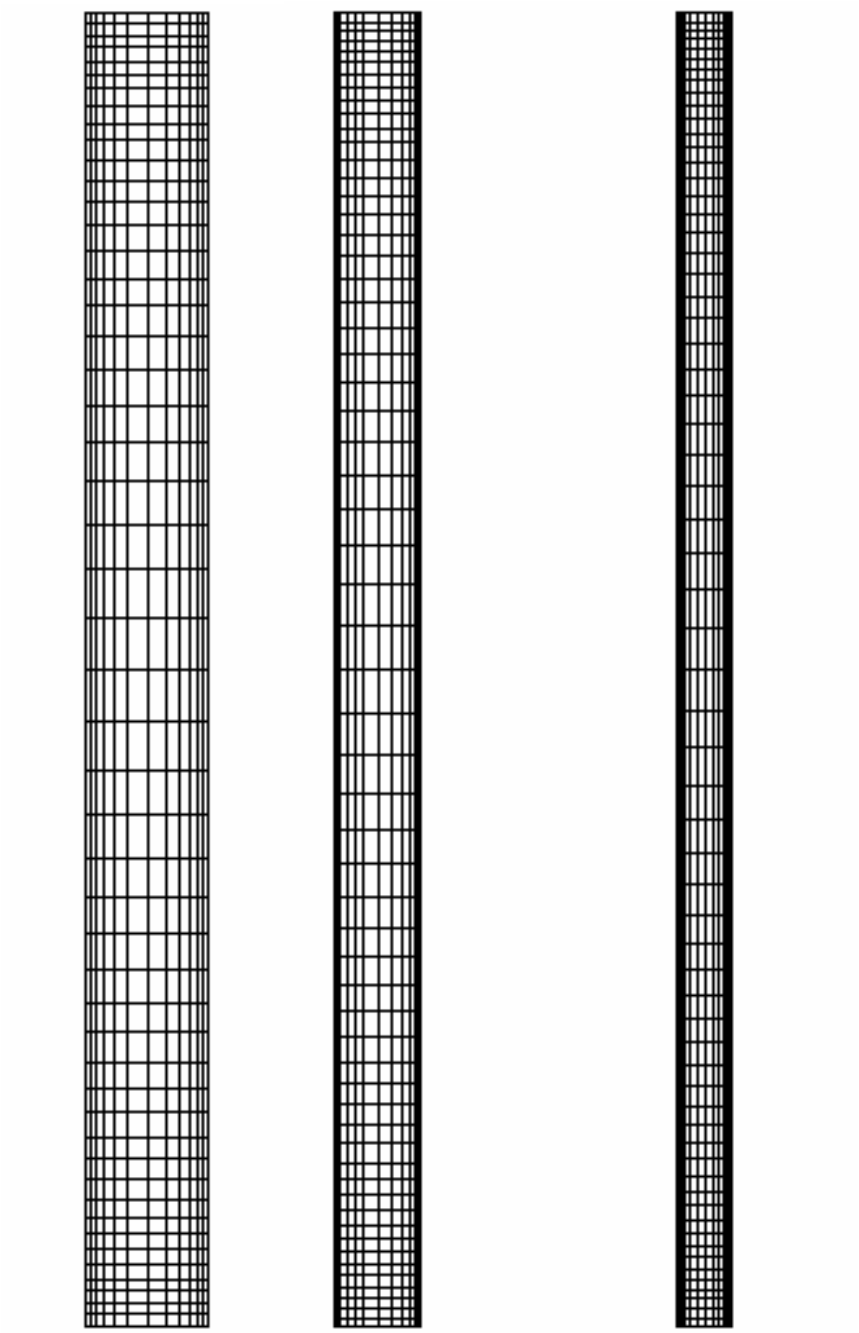

Figure 3. Examples of finite element meshs used.

RESULTS AND DISSCUSSION

The results obtained from the numerical solution for the IGU cavities have been plotted in Figure 4. For IGU cavities, the range of Ra_L typical for the majority of fenestration products is between 6000 and 10000 (Wright 1995), with some products having Ra_L up to 20000. Therefore, to more accurately predict the heat transfer across the IGU cavities, more data points are needed in that range, as indicated in Figure 4b.

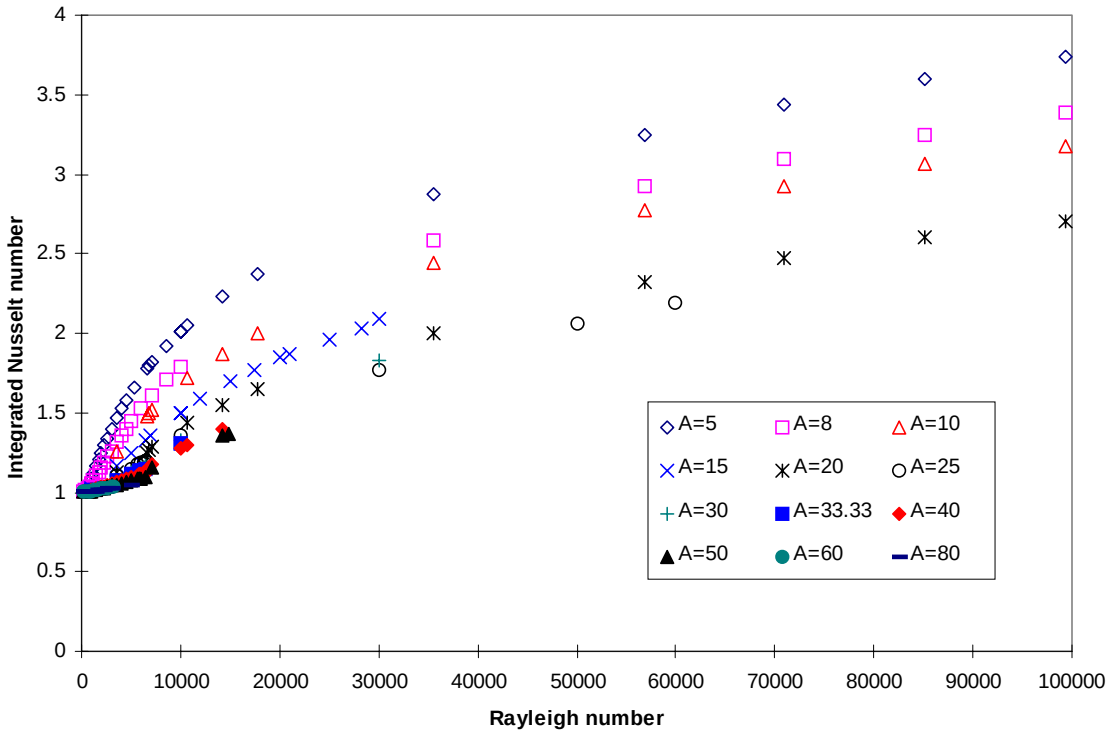

Figure 4 a. Results for IGU cavities over complete Ra_L range

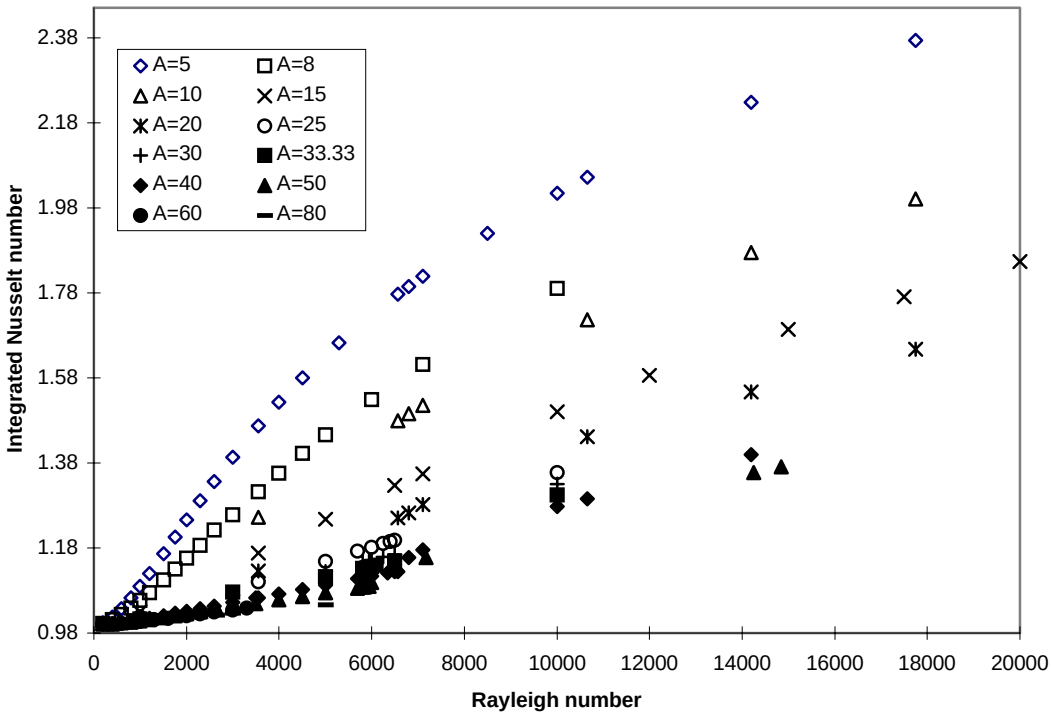

Figure 4b. Results for IGU cavities for $0 < Ra_L < 20000$

As mentioned earlier, the current study is restricted to the laminar flow regime. Therefore, as the aspect ratio increases, the range of data points that can be obtained becomes narrower as shown in Figure 4b. The results in Figure 4a were correlated by using the nonlinear fit algorithm given in Wolfram (1992) which resulted in the following two equations for A=5 to 80 and ZHF boundary conditions:

$$Nu = \begin{cases} [1 - 0.00813277 \times (\frac{Ra_L}{A}) + 0.00723291 \times (\frac{Ra_L}{A})^{1.08597}]^{0.279072}, & Ra_L < 10^4 \\ 0.0999542 \times (1 + 0.997983 \times e^{-0.0997981 \times A}) \times Ra_L{}^{0.274216}, & 10^4 \le Ra_L \le Ra_{ul} \end{cases} \quad (18)$$

Where Ra_{ul} is the upper limit of Ra_L for different aspect ratios as given in Figure 1. The correlation equations given in Equation 18 agree with the individual calculated results to within 6% (maximum deviation) and has a standard deviation was 2%. Equation 18 is not valid beyond the range of this numerical investigation (see Figure 1). This new correlation was then compared with existing correlations derived either from experimental data or from numerical data. These comparisons are shown in Figures 5 to 9 for aspect ratios from 5 to 80. Figures 5b, 6b and 7b show more detail in the typical fenestration Rayleigh number range.

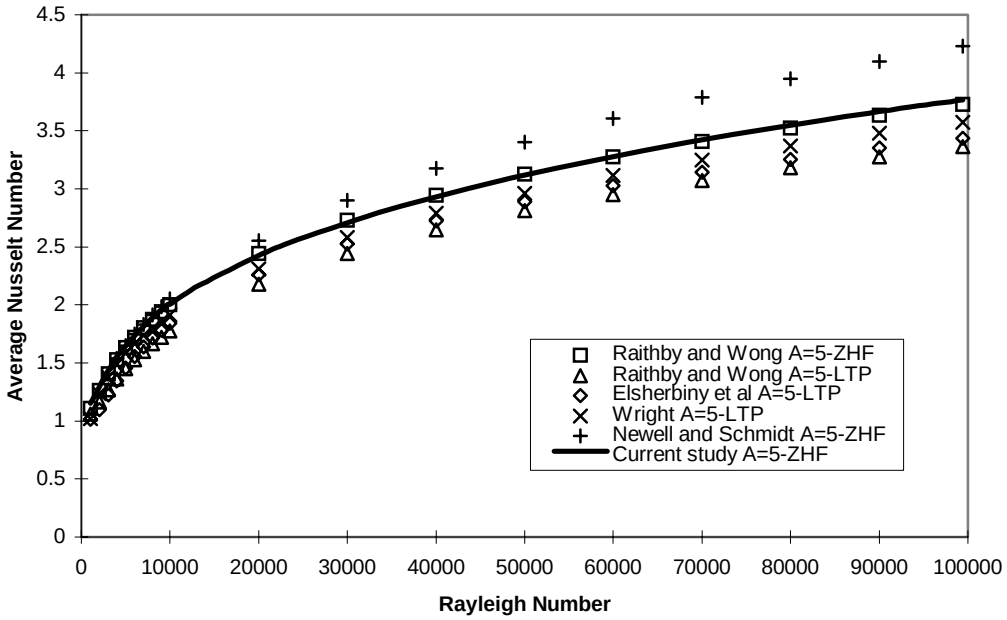

Figure 5a. Comparison of average Nu_L for aspect ratio = 5

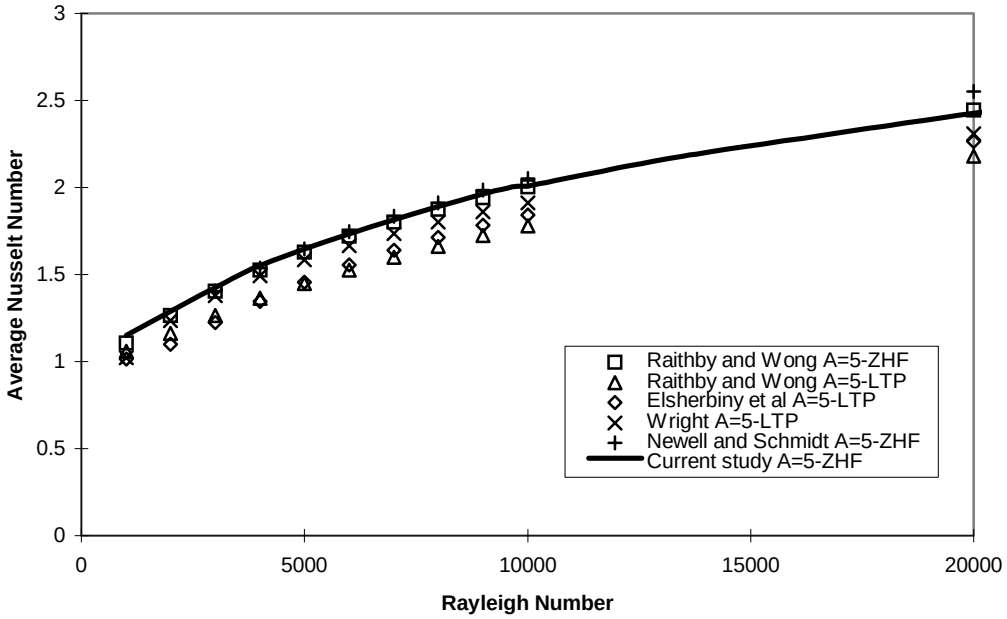

Figure 5b. Comparison of average Nu_L in the typical fenestration Ra_L range for A=5

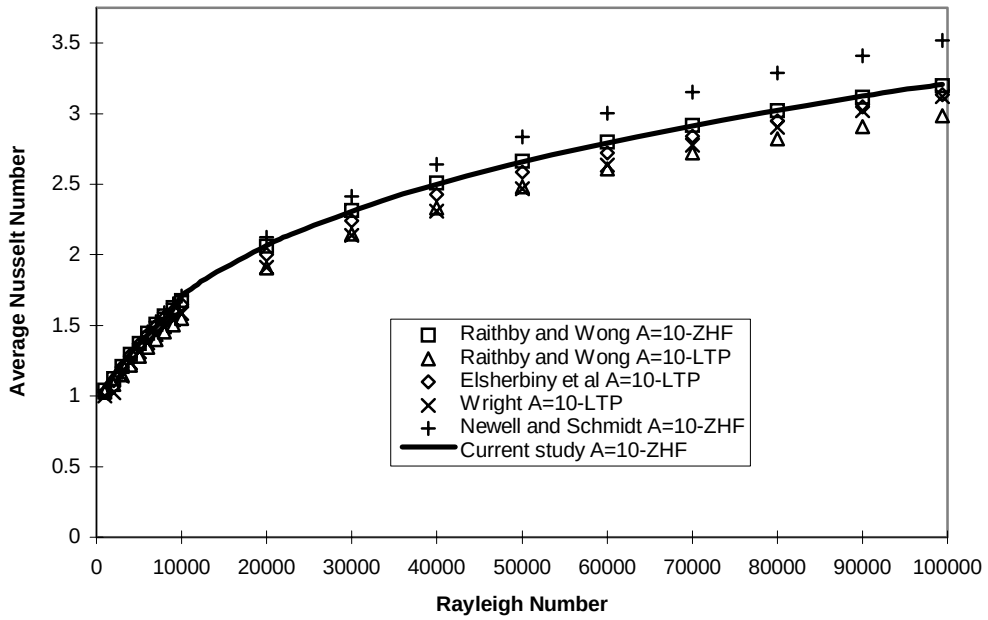

Figure 6a. Comparison of average Nu_L for aspect ratio = 10

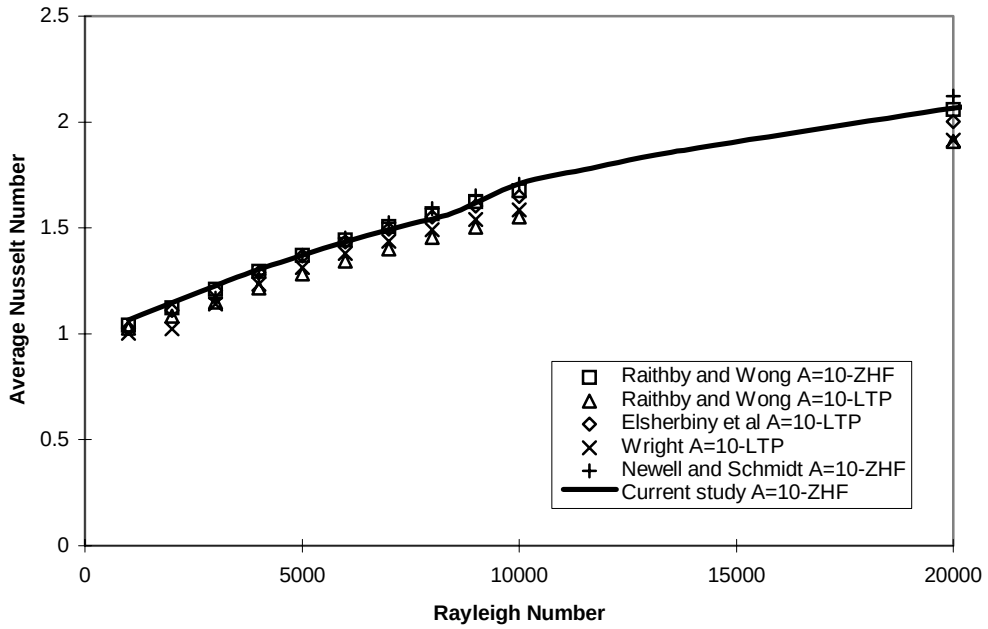

Figure 6b. Comparison of average Nu_L in the typical fenestration Ra_L range for A= 10

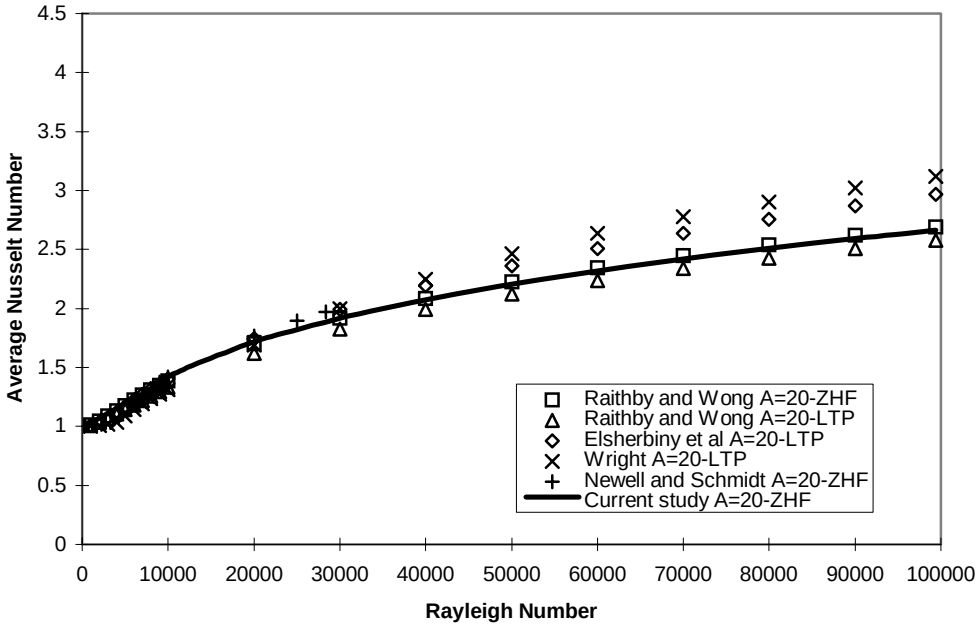

Figure 7a. Comparison of average Nu_L for aspect ratio = 20

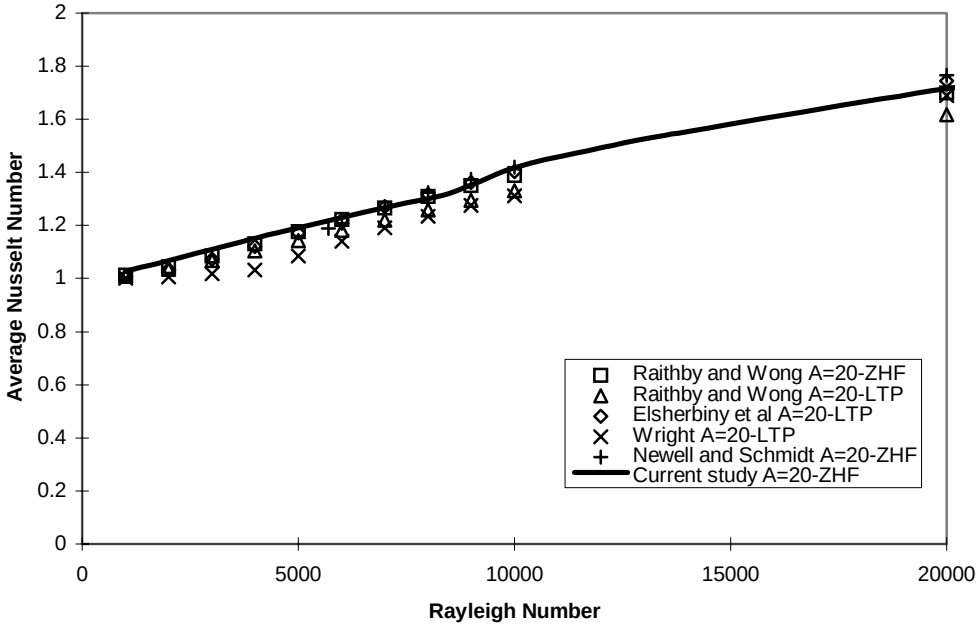

Figure 7b. Comparison of average Nu_L in the typical fenestration Ra_L range for A = 20

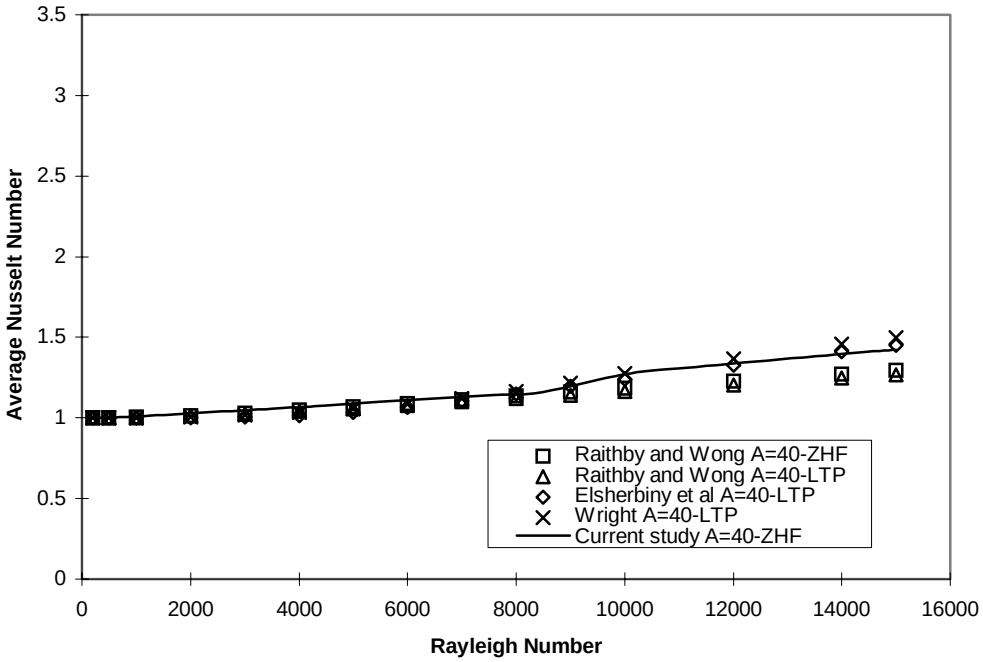

Figure 8. Comparison of average Nu_L for aspect ratio = 40

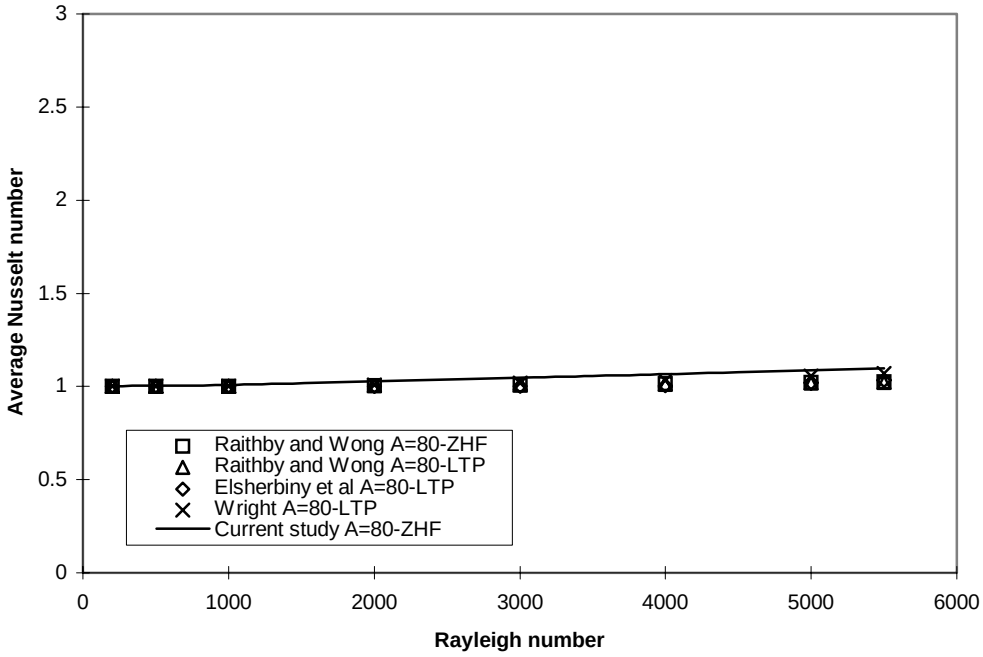

Figure9. Comparison of average Nu_L for aspect ratio = 80

Note that the symbols used represent the data points where the corresponding correlation was evaluated. All of the comparisons are made at the aspect ratio where the correlations of

ElSherbiny's "fine-grain structure" are available, since some or all of those five aspect ratios were also widely used in other numerical studies such as A=5, 10 and 20 in Newell and Schmidt's (1970) work and all of them by Raithby and Wong's (1981) study. In addition, it is also important to address the effect of the different thermal conditions applied on the top and bottom surfaces, which appears to be the reason for some of the disagreement between different researchers. Before doing this, it should be noted that the linear temperature profile (LTP) boundary condition more closely approximate the situation in a fenestration cavity with an aluminum spacer. The zero heat flux (ZHF) boundary condition is more representative of lower thermal conductivity spacer materials and geometries now being introduced by window manufacturers.

While this study and Newell and Schmidt (1970) and the ZHF correlation in Raithby and Wong (1981) uses ZHF boundary conditions on the top and bottom surfaces. ElSherbiny, et al (1982), Wright (1996) and the other set of correlations in Raithby and Wong (1981) are for the LTP boundary conditions on the top and bottom surfaces. Raithby and Wong (1981) showed that the trends to predict the heat transfer rate are similar for the ZHF and LTP conditions, but the value of the heat transfer is significantly lower for the LTP than the ZHF case for lower aspect ratios ($A \leq 40$), and the difference decreases as the aspect ratio increases. Wright (1990) also showed the existence of such a trend. By examining the ZHF results of current study with the LTP results of ElSherbiny, et al (1982) in Figures 5 to 9, except for A=20, this trend can also be observed. In the case of A=20, ElSherbiny's LTP correlation is consistently higher (up to 10 percent at Ra_L=99400) than Equation 18, a similar observation also applies to the correlation of Wright (1996), who developed a correlation based on measurements of both ElSherbiny, et al (1982) and Shewen (1986). Therefore, the influence of LTP and ZHF boundary conditions on the average Nu_L as shown in Figures 5 to Figure 9, in comparison with the other results, indicates that ElSherbiny's (1982) correlation overpredicts the actual Nu_L value at an aspect ratio A=20. At aspect ratio equal to 40 and 80 where it is believed that the influence of LTP and ZHF boundary conditions on Nu_L is small (Wright 1990), ElSherbiny's correlation agrees well with the current correlation as shown in Figure 8 and 9, having a maximum difference of 4 percent.

Contrary to ElSherbiny's LTP correlation developed from measured data, Raithby and Wong's numerical LTP correlation consistently predicts lower Nu_L than that of the current study for all of the aspect ratios under examination, with the deviations from 12% at A=5 to 1.6% at A=80 (see Figures 5 to 9). The ZHF correlation of Raithby and Wong, except for $Ra_L \geq 10000$ at A=40, is in general agreement with the correlation of current study with maximum difference of 2.4% occurring at A=20 and Ra_L=6000. For A=40 and $Ra_L \geq 10000$, Raithby and Wong's (1981) results produce differences in Nu_L up to 10 percent lower than Equation 18. The correlation equation of Newell and Schmidt (1970) agrees over their stated valid range to within 12% with Equation 18 (see Figures 5 to 7), with the largest deviations occurring at higher Ra_L. This is probably due to the form of their equation being simple power law equations which generally can not account for the complex interaction of A and Ra_L on Nu_L (see Figure 4).

CONCLUSIONS AND RECOMMENDATIONS

The new analytical correlation developed in this study resolves the dependence of Nu_L on both Rayleigh number and aspect ratio. From a large number of numerical calculations covering

a large range of aspect ratios and Rayleigh numbers, the calculated results provide enough information for developing a new correlation which is able to more accurately predict the heat transfer through the IGU cavities of fenestration products. The correlation compares favorably with the experiments results of ElSherbiny for A≥40, which are the typical of those found in fenestration products, where the influence of LTP and ZHF boundary conditions on Nu_L is small, and also with the numerical results of Raithby and Wong. The discrepancy existing between Equation 18 and the correlation of ElSherbiny, et al (1982) for lower aspect ratios (5,10) is due to the effect of the different thermal boundary conditions (LTP vs ZHF) imposed on the top and bottom surfaces.

Future work needs to include the linear temperature profile (LTP) boundary conditions for the same range of Ra_L and A, and to do additional numerical calculations in the range of 8000 to 10000 to obtain smoother transition between the two equations in the correlation (Equation 18). Also, the range of both A and Ra_L needs to be extended to include flows in the turbulent flow regime.

ACKNOLEDGEMENTS

This work was jointly sponsored by the Assistant Secretary for Conservation and Renewable Energy, Office of Buildings and Community Systems, Building Systems Division of the U.S. Department of Energy and the University of Massachusetts under Cooperative Agreement No. DE-FG03-94SF1812. Computations for large aspect ratios are carried out on CRAY C90 from the National Energy Research Scientific Computing Center at Lawrence Berkeley National Laboratory, under a grant from the U.S. Department of Energy.

NOMENCLATURE

A = aspect ratio, H/L
H = height of air layer (m)
L = thickness of air layer (m)
Nu_L = Integrated (or average) Nusselt number based on cavity thickness, hL/k
Pr = Prandtl number = 0.71, ν/α
Ra_L = Rayleigh number based on cavity thickness, $\frac{g\beta\Delta TL^3}{\nu\alpha}$
Gr_L = Grashof number based on cavity thickness, $\frac{g\beta\Delta TL^3}{\nu^2}$
T = temperature (K)
T_1 = temperature of cavity hot wall (K)
T_0 = temperature of cavity cold wall (K)
ΔT = temperature difference between cavity hot and cold wall (K)
u = x component of velocity (m/s)
v = y component of velocity (m/s)
c_p = Specific heat at constant pressure [J/kg·K]
g = Gravitational acceleration [m/s^2]
k = Thermal conductivity [W/m·K]
p = Total thermodynamic pressure [N/m^2]

α = Coefficient of thermal diffusion [m^2/s]
β = Coefficient of thermal expansion [1/K]
ΔT = Temperature difference [K]
Θ = Nondimensionless temperature [K]
μ = Dynamic viscosity [kg/m·s]
ρ = Density [kg/m^3]

REFERENCES

Batchelor, G. K. 1954. Heat Transfer by Free Convection Across a Closed Cavity Between Vertical Boundaries at Different Temperatures. Quarterly of Applied Mathematics12: 209-233.

Burnett, D. 1987. *Finite Element Analysis*. Addison-Wesley.

Curcija, D.1992 Three-dimensional Finite Element Model of Overall Nighttime Heat Transfer Through Fenestration Systems. Ph.D. dissertation, Amherst: University of Massachusetts.

Curcija, D., and Goss, W. P. 1993. Two-dimensional Natural Convection Over The Isothermal Indoor Fenestration Surface - Finite Element Numerical Solution. ASHRAE Transactions 99(1).

Curcija, D., and Goss, W. P. 1994. Two-dimensional Finite Element Model of Heat Transfer in Complete Fenestration Systems. ASHRAE Transactions 100(2).

Eckert, E. R. G. and Carlson, W. O. 1961. Natural Convection in an Air Layer Enclosed Between Two Vertical Plates with Different Temperatures. International Journal of Heat and Mass Transfer, Vol. 2, pp.106-120.

Elder, J. W. 1965. Laminar Free Convection in A Vertical Slot. Journal of Fluid Mechanics 23: 77-98.

ElSherbiny, S. M., Raithby, G. D., and Hollands, K. G. T. 1982. Heat Transfer by Natural Convection Across Vertical And Inclined Air Layers. ASME Journal of Heat Transfer, Vol. 104, pp. 96-102.

FDI. 1996. *FIDAP* 7.0 --- User's and reference manual. Evanston, Ill.: Fluid Dynamics International.

Gill, A. E. 1966. The Boundary-layer Regime for Convection in A Rectangular Cavity. Journal of Fluid Mechanics, Vol. 26, pp. 515-536.

Jakob, M. 1967. *Heat Transfer*, Vol. 1, Wiley, New York, 1967, pp. 536-539.

Korpela, S. A. et al. 1982. Heat Transfer Through A Double Pane Window. ASME Journal of Heat Transfer, Vol. 104, pp. 539-544.

Le Quéré, P. 1990. A Note on Multiple and Unsteady Solutions in Two-Dimensional Convection in A Tall Cavity. Journal of Heat Transfer, Vol. 112, pp. 965-974.

Lee, Y., and Korpela, S. A.1983. Multicellular Natural Convection In A Vertical Slot. Journal of Fluid Mechanics, Vol. 126, pp. 91-121.

Newell, M.E., and Schmidt, F.W. 1970. Heat Transfer by Laminar Natural Convection Within Rectangular Enclosures. Journal of heat Transfer, Vol. 92, pp. 159-165.

Raithby, G.D., and Hollands, K.G.T., 1975. A General Method of Obtaining Approximate Solutions to Laminar and Turbulent Free Convection Problems. *Advances in Heat Transfer*, Vol. 11, pp. 265-315.

Raithby, G.D., Hollands, K.G.T., and Unny, T. 1977. Analysis of Heat Transfer by Natural Convection Across Vertical Fluid Layers. Journal of Heat Transfer, Vol. 99, pp. 287-293.

Raithby, G.D., and Wong, H.H. 1981. Heat Transfer by Natural Convection Across Vertical Air Layers. Numerical Heat Transfer, Vol. 4, pp. 447-457.

Shewen, E. C. 1986. A Peltier Effect Technique for Natural Convection Heat Flux Measurement Applied to the Rectangular Open Cavity. Ph.D. thesis, Dept. of Mechanical Engineering. Waterloo, ON: University of Waterloo, Canada.

Wright, J.L. 1990. The Measurement and Computer Simulation of Heat Transfer in Glazing Systems. Ph.D. dissertation, Department of Mechanical Engineering, Waterloo, ON: University of Waterloo.

Wright, J.L., Sullivan, H.F., 1995. A Simplified Method for the Numerical Condensation Resistance Analysis of Windows, Window Innovations'95, Toronto, Canada, June 5, 6 (1995).

Wright, J.L. 1996. A Correlation to Quantify Convective Heat Transfer Between Vertical Window Glazings. ASHRAE Transactions 102 (1).

Yin, S. H., Wung, T. Y., and Chen, K. 1978. Natural Convection in An Air Layer Enclosed Within Rectangular Cavities. International Journal of Heat and Mass Transfer, Vol. 21, pp. 307-315.

Zhao,Y., D. Curcija, and W.P. Goss. 1997. Prediction of the Multicellular Flow Regime of Natural Convection in Fenestration Glazing Cavities. ASHRAE Transactions 103 (1).